

Threshold Stress Intensity Factor in Soda–Lime Silicate Glass by Interrupted Static Fatigue Test

Vincenzo M. Sglavo & David J. Green*

Department of Materials Science and Engineering, The Pennsylvania State University, University Park, PA 16802, USA

(Received 15 August 1994; accepted 9 September 1995)

Abstract

The measurement of the threshold stress intensity factor K_{th} for sub-critical crack growth of soda–lime glass in a water environment was performed using the interrupted static fatigue test. The experimental procedures suggested in a previous paper by the current authors were followed. In the first approach, K_{th} was calculated as the stress intensity factor at which half of the specimens fail during the constant stress phase of the test. In the second approach, the fatigue limit was determined from the stress intensity factor applied to the weakest surviving sample during the stress hold. For both cases, values of the stress intensity factor were obtained for increasing hold times, which ranged from 1 hour to 20 days. The estimated K_{th} values decrease with holding time but are expected to reach a limiting value, equivalent to the true threshold at long times. For holding times of 20 days, values of 0.16 and 0.15 MPa m^{1/2} were obtained by using the two different approaches. For the current test, the necessary limit in the estimated K_{th} values was not obtained, suggesting that if a threshold exists, it must be equal to or less than these values. These values are significantly lower than previous K_{th} estimates that were obtained by extrapolation from crack velocity and time-to-failure measurements (0.2–0.4 MPa m^{1/2}).

1 Introduction

Sub-critical crack growth in silicate glasses is a well-known phenomenon. As a result of such behaviour, the strength depends on loading time and environmental conditions and this fatigue effect has been extensively studied. Some works have shown that this sub-critical behaviour seems to possess a lower limit, in the sense that the crack propagation velocity tends to zero for some par-

ticular value of the applied stress intensity factor.^{1–8} This value is termed the fatigue limit or the threshold stress intensity factor. From an engineering design point of view, the existence of a fatigue limit turns out to be extremely desirable, as it allows an applied stress to be defined, below which delayed failure does not occur. The determination of the fatigue limit is therefore of practical importance and this effect has aroused the interest of many researchers.

In early works on sub-critical crack growth in silicate glasses, samples were loaded at different stress levels in bending and the lifetimes were measured.^{9–17} The 'endurance limit' was defined as the stress at which the fatigue curve shows asymptotic behaviour. For soda–lime glass in a water environment, values ranging from 0.15 to 0.4 times the strength measured in liquid nitrogen were extrapolated from time-to-failure measurements.^{10–16} The same approach, used in more recent work by Pavelchek and Doremus¹⁸ and Gehrke *et al.*,^{19–21} furnished similar results.

Studies devoted to sub-critical crack growth velocity determination as a function of the applied stress intensity factor also showed, in some cases, the existence of a threshold below which crack motion did not occur. In these studies, double cantilever beam and double torsion fracture mechanics geometries were often used and crack advancement was measured as a function of time. Values of the threshold ranging from 0.18 to 0.40 MPa m^{1/2} were put forward.^{1–8,22} It must be pointed out, in these cases, that the fatigue limit corresponded to a value extrapolated from crack velocity measurements.

Although a significant number of studies have been performed, definitive proof for the existence of a fatigue limit is still an open problem and many uncertainties are present. For example, Simmons and Freiman⁵ observed crack arrest in soda–lime glass in water at stress intensity factor of 0.27 MPa m^{1/2} but they defined this threshold as an 'apparent' effect, because it was not associated

*To whom correspondence should be addressed.

with crack tip blunting, as predicted by the theory of Hillig and Charles.¹⁷ Conversely, Michalske demonstrated the occurrence of crack tip blunting for stress intensity factors lower than $0.25 \text{ MPa m}^{1/2}$ using crack ageing experiments.²³

In a previous paper,²⁴ a theoretical analysis of the interrupted static fatigue (ISF) test was developed. This test has been used previously for the determination of the fatigue limit in various glass and ceramic materials.^{25–31} In the theoretical analysis,²⁴ some procedures were proposed for the correct evaluation of the threshold. In the current paper, the measurement of the fatigue limit in soda-lime silicate glass in water environment was attempted on the basis of these procedures.²⁴

2 Experimental Procedure

Soda-lime silicate glass rods from a commercial source (0080 Code, Corning Glass Works) were used in this work. The composition of the glass is reported in Table 1. The rods, with a nominal diameter of 3.2 mm, were cut into 90 mm length samples and these were annealed at 520°C for 24 h in order to remove any residual stress. Heating and cooling rates of below 1°C min^{-1} were used for this purpose.

Inert strengths were determined by a four-point bend test performed in paraffin oil. Samples were initially stored in a furnace at $\sim 120^\circ\text{C}$ for 15 min and then immediately immersed in a paraffin oil bath. The bend fixture, with outer and inner spans of 80 and 20 mm, respectively, was also completely immersed in an oil bath, as shown in Fig. 1. In this way, the inert conditions were maintained during the testing of the glass rods. A crosshead speed of 15 mm min^{-1} was used for these tests. Forty rods were used for strength determination and the diameter of each sample was measured, after failure, close to the fracture surface.

The strength of 40 samples was also measured in water environment at the same crosshead speed as in the inert measurements. For these tests, the four-point fixture was immersed in a deionized water bath (Fig. 1).

The interrupted static fatigue tests were performed in a deionized water bath (pH 6.0–6.5). A constant load was applied to groups of eight samples using free-hanging weights. A schematic of the apparatus used for the ISF test is shown in Fig. 2. The glass samples were placed on two

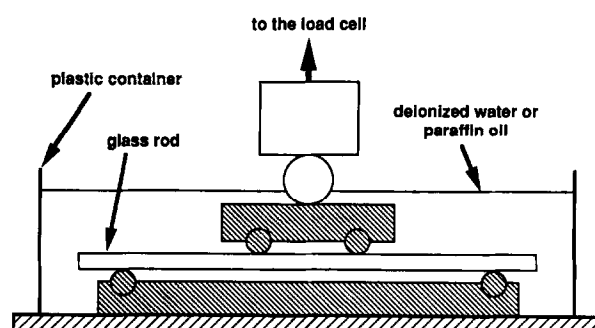


Fig. 1. Schematic of the four-point bending fixture used for strength testing in paraffin oil and in deionized water.

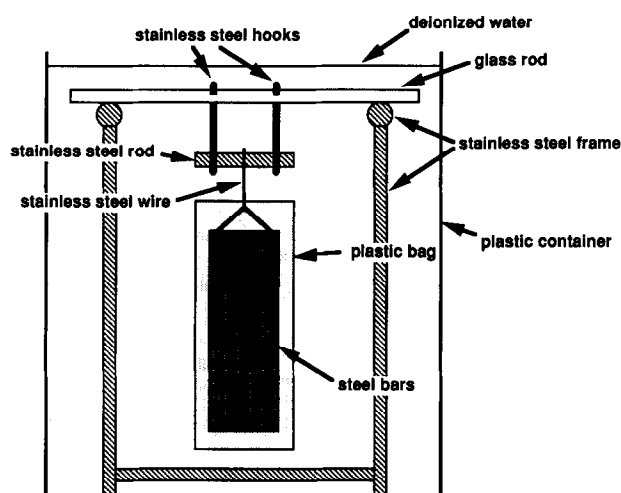


Fig. 2. Schematic of the apparatus used for the ISF test.

stainless steel rods which were suspended by a stainless steel frame. The load was applied in a four-point bend configuration by use of the two hooks. Outer and inner spans were again 80 and 20 mm, respectively. Great care was taken to avoid any contact of the hooks with the rods before the final loading. The hanging weights consisted of a set of steel bars to obtain the desired load. To avoid any contamination of the deionized water from the steel bars, each weight set was contained in a plastic bag which was carefully closed and sealed with silicone grease. The constant load was maintained on the specimens for times ranging from 1 h to 20 days. Care was taken to account for the buoyancy force acting on the steel bars, in the evaluation of the applied stress. Samples which did not fail during the constant phase of the testing were then broken in four-point bending using the same procedure as that described for the strength determination in water. Before this final testing, samples were marked on their edge in order to load them in the same orientation that was used during the static hold.

Table 1. Composition (wt%) of the soda-lime silicate glass used in the present work

SiO_2	Al_2O_3	MgO	CaO	Na_2O	K_2O	BaO	B_2O_3	Other
68.1	2.2	3.8	5.7	15.5	0.7	1.9	1.5	0.6

3 Analysis of Results and Discussion

Figure 3 shows the Weibull plot for the strength distributions determined in paraffin oil and in water. Failure probability F of each specimen was determined from the relationship:

$$F = \frac{j}{N + 1} \quad (1)$$

where j is the rank in the ascending distribution and N is the total number of specimens which, in this case, is equal to 20.

The sub-critical crack growth phenomenon is responsible for a marked decrease in strength when the testing is performed in an active environment, even with the high stressing rates used in this study ($\sim 47 \text{ MPa s}^{-1}$). A Weibull modulus of 5.5 was determined by linear regression of the inert strength data shown in Fig. 3.

In a previous paper,²⁴ Sglavo and Green suggested two different approaches to measure the threshold for sub-critical crack growth K_{th} by the ISF test. In the first approach the estimate of K_{th} is calculated as the stress intensity factor at which 50% of the samples fail during the stress hold. In the second approach, the fatigue limit is estimated as the stress intensity factor corresponding to the weakest specimen in the strength distribution of samples that survive the hold stress. It was pointed out that the second approach is preferred for materials with low Weibull modulus. In this work, even if the second approach would be more opportune, the threshold measurement was attempted using both procedures. For both procedures, a critical facet of the approach is to determine the K_{th} estimates as a function of hold time.²⁴

Figure 4 shows the strength S_1 measured in water, after the hold, as a function of the applied stress σ for holding times varying from 1 h to 20 days. The number of samples surviving and failing during the ISF test is also shown. The strength of the surviving specimens, S_1 , is substantially equivalent to the strength measured in water on

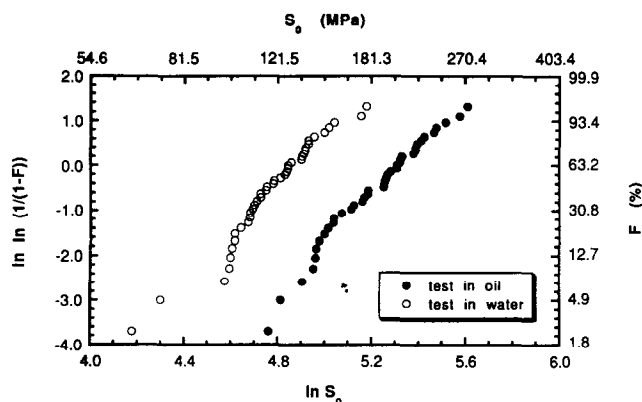


Fig. 3. Weibull plot of the strength distributions measured in paraffin oil and in deionized water.

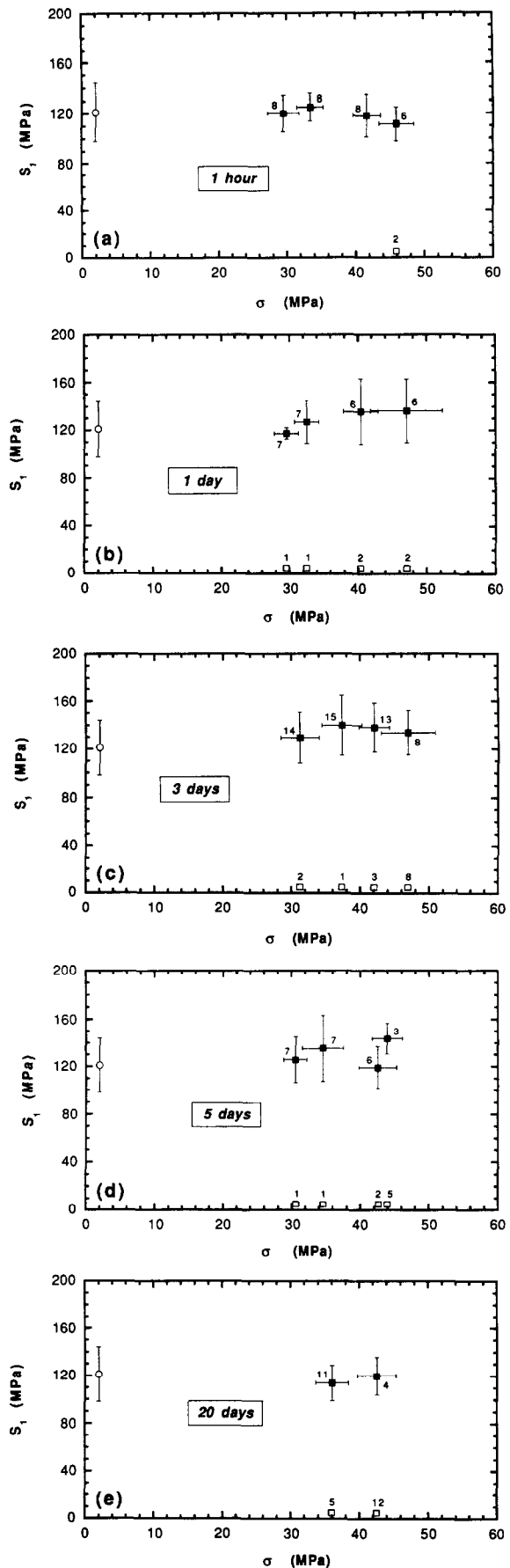


Fig. 4. Average strength S_1 measured in deionized water, after the hold, as a function of the applied stress σ for holding times of (a) 1 h, (b) 1 day, (c) 3 days, (d) 5 days and (e) 20 days. Initial strength S_0 , measured in water, is shown at $\sigma = 2 \text{ MPa}$ for comparison. The error bars represent the standard deviation of the data. Empty square symbols correspond to specimens which failed during the stress hold. Each symbol is marked by the corresponding number of specimens.

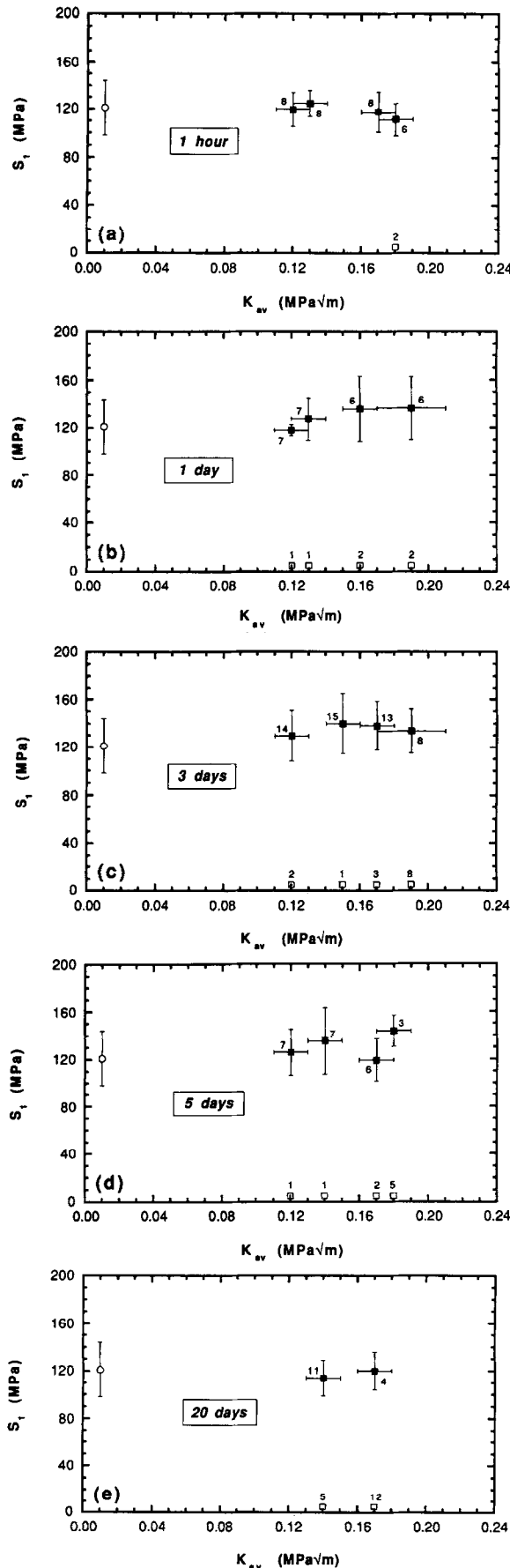


Fig. 5. Average strength S_I measured in deionized water, after the hold, as a function of K_{av} for holding times of (a) 1 h, (b) 1 day, (c) 3 days, (d) 5 days and (e) 20 days. Initial strength S_0 , measured in water, is shown at $K_{av} = 0.01 \text{ MPa m}^{1/2}$ for comparison. The error bars represent the standard deviation of the data. Empty square symbols correspond to specimens which failed during the stress hold. Each symbol is marked by the corresponding number of specimens.

as-annealed samples. Some variations, probably connected to the small number of samples used in this testing, can be detected. The average stress intensity factor K_{av} applied to the samples during the hold can be calculated as:²⁴

$$K_{av} = K_c \left(\frac{\sigma}{S_0} \right) \quad (2)$$

where S_0 is the average inert strength and K_c represents the fracture toughness, assumed to be equal to $0.75 \text{ MPa m}^{1/2}$ (Ref. 32). Figure 5 shows strength results of Fig. 4 as a function of K_{av} . As suggested in our previous paper,²⁴ the 'potential' threshold is first estimated as the value of the stress intensity factor, $(K_{av})_{50\%}$, at which 50% of samples fail during the hold. Due to the particular stresses used in this work, $(K_{av})_{50\%}$ could not be calculated for holding times of 1 h and 1 day. For these two cases, only values larger than $0.18 \text{ MPa m}^{1/2}$ could be assumed for $(K_{av})_{50\%}$. In order to take into account the scatter shown by the applied stress and, more importantly, by the inert strength, the average value of $(K_{av})_{50\%}$ was calculated, more precisely, according to the following relationship:³³

$$(K_{av})_{50\%} = K_c \left(\frac{\sigma_{50\%}}{S_0} \right) + \frac{K_c \sigma_{50\%}}{S_0^3} V(S_0) \quad (2a)$$

where $\sigma_{50\%}$ is the applied stress corresponding to 50% of failures during the holding and $V(S_0)$ represents the variance of the inert strength, i.e. the square of the standard deviation.³³ The second term in eqn (2a), usually very small, is related to the transformation used to calculate $(K_{av})_{50\%}$ from σ and S_0 , both of which are random variables.³³ Analogously, the standard deviation $[V((K_{av})_{50\%})]^{1/2}$ was calculated from:³³

$$[V((K_{av})_{50\%})]^{1/2} = \left[\left(\frac{K_c}{S_0} \right)^2 V(\sigma_{50\%}) + \left(\frac{K_c \sigma_{50\%}}{S_0^3} \right)^2 V(S_0) \right]^{1/2} \quad (2b)$$

where $V(\sigma_{50\%})$ represents the variance of the applied stress corresponding to 50% of failures. $\sigma_{50\%}$ can be calculated by linear interpolation between two distinct applied stress values, σ_2 and σ_1 , corresponding to the percentages of specimens failing during the stress hold, n_1 and n_2 , with $n_1 < 0.5 < n_2$. The variance $V(\sigma_{50\%})$ was evaluated as:³³

$$V(\sigma_{50\%}) = \left(\frac{0.5 - n_1}{n_2 - n_1} \right) V(\sigma_2) + \left(\frac{n_2 - 0.5}{n_2 - n_1} \right) V(\sigma_1) \quad (2c)$$

where $V(\sigma_1)$ and $V(\sigma_2)$ represent the variance of the two applied stress values used in the interpolation. The results of these calculations are shown in Fig. 6. As was expected, a large scatter is shown by the stress intensity values, due to the low

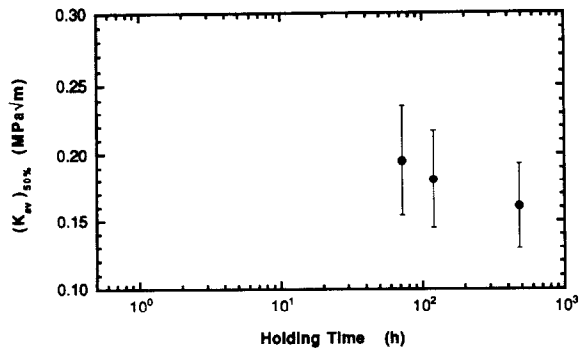


Fig. 6. $(K_{av})_{50\%}$ as a function of the holding time as calculated on the basis of the results shown in Fig. 5. The error bars represent the standard deviation of the data and are discussed in the text.

Weibull modulus associated with the inert strength. Nevertheless, a general trend is evident in Fig. 6: $(K_{av})_{50\%}$ decreases for increased holding times. A value of $0.16 \pm 0.03 \text{ MPa m}^{1/2}$ is obtained at $t = 20$ days for the K_{th} estimate. It is important to note that $(K_{av})_{50\%}$ has not reached an invariant limit for this hold time, as required in the proper determination of K_{th} .²⁴

An alternative approach to the determination of the fatigue threshold was performed by considering the strength distribution of samples that survive the hold stress.²⁴ Figure 7 shows the strength distributions corresponding to different holding times. A failure strength equal to zero was assigned to samples which failed during the stress hold. For each holding time, the data corresponding to the two upper applied stress shown in Fig. 4 were analysed. The weakest survivor in each distribution was considered and its inert strength S_{0w} was calculated from the data shown in Fig. 3, on the basis of its failure probability. The stress intensity factor K_w applied to this weakest surviving sample was calculated as:

$$K_w = K_c \left(\frac{\sigma}{S_{0w}} \right) \quad (3)$$

where σ is again the applied stress during the hold. Figure 8 shows the results of these calculations. The stress intensity factor applied to the specimens directly preceding and following the weakest sample in the ascending strength distribution is also shown in Fig. 8. In this way, an estimate of the possible computation error can be furnished. K_w decreases for increased holding times and for $t \geq 72$ h the trend is similar to that shown in Fig. 6. For a holding time of 480 h, K_w assumes a value of $\sim 0.15 \text{ MPa m}^{1/2}$ but, again, no invariance is seen in K_w for the longer hold times.

The two approaches used to determine the 'potential' threshold furnished similar results. Both $(K_{av})_{50\%}$ and K_w decrease for increased holding times, according to the arguments pointed out

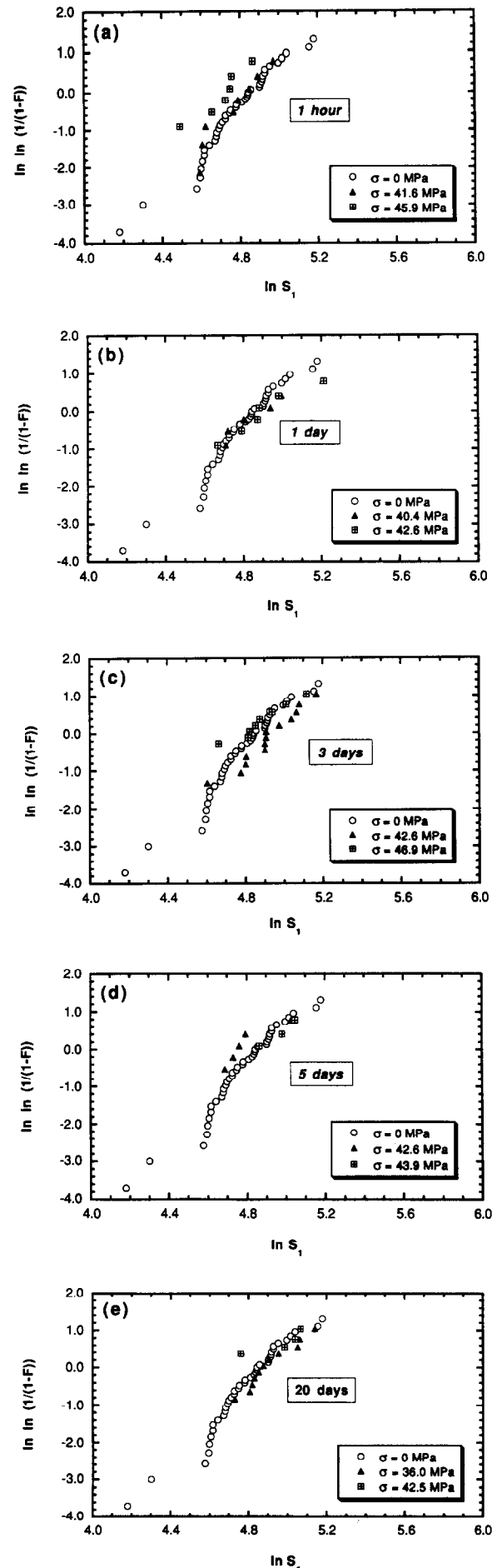


Fig. 7. Strength distribution evaluated after the stress hold, for holding times of (a) 1 h, (b) 1 day, (c) 3 days, (d) 5 days and (e) 20 days. The initial strength distribution, measured in deionized water, is shown for comparison ($\sigma = 0$ MPa).

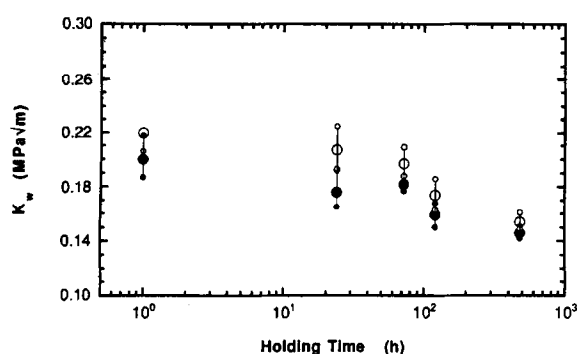


Fig. 8. Stress intensity factor K_w applied to the weakest specimen of the strength distributions shown in Fig. 7 as a function of the holding time. Empty symbols correspond to the highest applied stress defined in Fig. 7. The smaller symbols represent the stress intensity factor applied to the specimens directly preceding and following the weakest specimen in the ascending strength distribution.

previously.²⁴ These two parameters seem to be approaching a limiting value around 0.14–0.15 MPa m^{1/2} though the holding times used in this work are not long enough to be conclusive on this point. Nevertheless, results of Figs 6 and 8 lead to some important considerations.

First of all, values of the 'potential' threshold for soda-lime glass presented in this work are lower than the fatigue limit extrapolated from crack velocity measurements and reported by other authors.^{1–4,6–8} Values of K_{th} ranging from 0.18 to 0.40 MPa m^{1/2} have been proposed for soda-lime glass in water environment.^{1–4,6–8} Results of this work show a better agreement with data presented in early works on static fatigue of soda-lime glass where the 'endurance limit' was assumed as the stress equal to 0.2–0.4 times the strength measured in liquid nitrogen.^{10,11,14,16} These values correspond to a stress intensity factor of 0.15–0.30 MPa m^{1/2}. On the basis of the arguments pointed out by Sglavo and Green,²⁴ measurement of the real value of the fatigue limit from an ISF test would require even longer hold times. The decision to use such long hold times would depend on various factors like experimental costs and the importance of the threshold information in component design.

4 Conclusions

The interrupted static fatigue test was used to determine the threshold for sub-critical crack growth in soda-lime silicate glass in water environment. The two procedures described in a previous paper were followed. First of all, the 'potential' fatigue limit was calculated as the stress intensity factor at which 50% of samples fail during the static hold for different hold times. In a second approach, K_{th} was determined as the value

of the stress intensity factor applied to the weakest specimen in the strength distribution that survived the stress hold. Holding times ranging from 1 h to 20 days were used and 'potential' threshold values appeared to decrease for longer times. Theoretical calculation had shown that the estimates could be considered to be threshold values if they become invariant with hold time. Values of 0.16 and 0.15 MPa m^{1/2} were obtained by the two different procedures at holding times of 20 days. Unfortunately, although an asymptotic behaviour was shown by the calculated threshold values, invariance with hold time was not shown. Nevertheless, values of K_{th} calculated at 20 days are lower than fatigue limit values presented in previous works for soda-lime glass in water environment. Only the use of longer holding times would allow a more precise evaluation of the threshold.

References

1. Wiederhorn, S. M. & Bolz, L. H., Stress corrosion and static fatigue of glass. *J. Am. Ceram. Soc.*, **53** (10) (1970) 543–8.
2. Evans, A. G., A simple method for evaluating slow crack growth in brittle materials. *Int. J. Fract.*, **9** (3) (1973) 267–75.
3. Wiederhorn, S. M., Subcritical crack growth in ceramics. In *Fracture Mechanics of Ceramics*, ed. R. C. Bradt, D. P. H. Hasselmann & F. F. Lange. Plenum, New York, 1974, Vol. 2, pp. 613–46.
4. Evans, A. G., Slow crack growth in brittle materials under dynamic loading conditions. *Int. J. Fract.*, **10** (2) (1974) 251–9.
5. Simmons, C. J. & Freiman, S. W., Effect of corrosion processes on subcritical crack growth in glass. *J. Am. Ceram. Soc.*, **64** (11) (1981) 683–6.
6. Wan, K., Lathabai, S. & Lawn, B. R., Crack velocity functions and threshold in brittle solids. *J. Eur. Ceram. Soc.*, **6** (1990) 259–68.
7. Gehrke, E., Ullner, C. & Hähner, M., Effect of corrosive media on crack growth of model glasses and commercial silicate glasses. *Glastech. Ber.*, **63**(9) (1990) 255–65.
8. Gehrke, E., Ullner, C. & Hähner, M., Fatigue limit and crack arrest in alkali-containing silicate glasses. *J. Mater. Sci.*, **26** (1991) 5445–55.
9. Stuart, D. A. & Anderson, O. L., Dependence of ultimate strength of glass under constant load on temperature, ambient atmosphere, and time. *J. Am. Ceram. Soc.*, **36** (12) (1953) 416–24.
10. Shand, E. B., Experimental study of fracture of glass: I, The fracture process. *J. Am. Ceram. Soc.*, **37** (2) (1954) 52–60.
11. Mould, R. E. & Southwick, R. D., Strength and static fatigue of abraded glass under controlled ambient conditions: II, Effect of various abrasions and the universal fatigue curve. *J. Am. Ceram. Soc.*, **42** (12) (1959) 582–92.
12. Mould, R. E., Strength and static fatigue of abraded glass under controlled ambient conditions: III, Aging of fresh abrasions. *J. Am. Ceram. Soc.*, **43** (3) (1960) 160–7.
13. Shand, E. B., Fracture velocity and fracture energy of glass in the fatigue range. *J. Am. Ceram. Soc.*, **44** (1) (1961) 21–6.
14. Mould, R. E., Strength and static fatigue of abraded glass under controlled ambient conditions: IV, Effect of surrounding medium. *J. Am. Ceram. Soc.*, **4** (10) (1961) 481–91.

15. Watanabe, M., Caporali, R. V. & Mould, R. E., The effect of chemical composition on the strength and static fatigue of soda-lime glass. *Phys. Chem. Glasses*, **2** (1) (1961) 12–23.
16. Shand, E. B., Strength of glass — the Griffith method revised. *J. Am. Ceram. Soc.*, **48** (1) (1965) 43–9.
17. Hillig, W. B. & Charles, R. J., Surfaces, stresses-dependent surface reactions, and strength. In *High Strength Materials*, ed. V.F. Zakay. John Wiley & Sons, New York, 1965, pp. 683–705.
18. Pavelchek, E. K. & Doremus, R. H., Static fatigue in glass — a reappraisal. *J. Non-Cryst. Solids*, **20** (1976) 305–21.
19. Gehrke, E., Ullner, C. & Hähner, M., Strength and fatigue of some binary and ternary silicate glasses. *J. Non-Cryst. Solids*, **80** (1986) 269–76.
20. Gehrke, E., Ullner, C. & Hähner, M., Correlation between multistage crack growth and time-dependent strength in commercial silicate glasses. Part 1. Influence of ambient media and types of initial cracks. *Glastech. Ber.*, **60** (8) (1987) 268–78.
21. Gehrke, E., Ullner, C. & Hähner, M., Correlation between multistage crack growth and time-dependent strength in commercial silicate glasses. Part 2. Influence of surface treatment. *Glastech. Ber.*, **60** (10) (1987) 340–5.
22. Evans, A. G., A method for evaluating the time-dependent failure characteristics of brittle materials — and its application to polycrystalline alumina. *J. Mater. Sci.*, **7** (1972) 1137–46.
23. Michalske, T. A., The stress corrosion limit: its measurement and implications. In *Fracture Mechanics of Ceramics*, ed. R. C. Bradt, D. P. H. Hasselmann & F. F. Lange. Plenum Press, New York, 1983, Vol. 5, pp. 277–89.
24. Sglavo, V. M. & Green, D. J., The interrupted static fatigue test for evaluating threshold stress intensity factor in ceramic materials: a theoretical analysis. *J. Eur. Ceram. Soc.*, **15** (1995) 777–86.
25. Wilkins, B. J. S. & Dutton, R., Static fatigue limit with particular reference to glass. *J. Am. Ceram. Soc.*, **59** (3–4) (1975) 108–12.
26. Minford, E. J. & Tressler, R. E., Determination of threshold stress intensity for crack growth at high temperature in silicon carbide ceramics. *J. Am. Ceram. Soc.*, **66** (5) (1983) 338–40.
27. Minford, E. J., Kupp, D. M. & Tressler, R. E., Static fatigue limit for sintered silicon carbide at elevated temperatures. *J. Am. Ceram. Soc.*, **66** (11) (1983) 769–73.
28. Foley, M. R. & Tressler, R. E., Threshold stress intensity for crack growth at elevated temperatures in a silicon nitride ceramic. *Adv. Ceram. Mater.*, **34** (1988) 383–6.
29. Yavuz, B. O. & Tressler, R. E., Threshold stress intensity for crack growth in silicon carbide ceramics. *J. Am. Ceram. Soc.*, **76**(4) (1993) 1017–24.
30. Hayashi, K., Easler, T. E. & Bradt, R. C., A fracture statistics estimate of the fatigue limit of a borosilicate glass. *J. Eur. Ceram. Soc.*, **12** (1993) 487–91.
31. Ogasawara, T., Hori, T. & Okada, A., Threshold stress intensity for oxidative crack healing in sintered silicon nitride. *J. Mater. Sci. Lett.*, **13** (1994) 404–6.
32. Wiederhorn, S. M., Fracture surface energy of glass. *J. Am. Ceram. Soc.*, **52** (1969) 99–105.
33. Hahn, G. J. & Shapiro, S. S., *Statistical Models in Engineering*. John Wiley & Sons, New York, 1967.